

NUMERICAL STUDIES OF MICROCATHODE SUSTAINED DISCHARGE FOR GENERAL ENGINEERING APPLICATION

R. K. Das¹, Umme Mumtahina² and A. S. M Sayem³

¹Institute of E-vehicle Technology, University of Ulsan, Ulsan 680-749, Korea

²Department of Electrical and Electronic Engineering, Chittagong University of Engineering & Technology

³Chittagong University of Engineering & Technology, Chittagong

^{1,*}ratanme06_cuet@yahoo.com, ²mumtahina58eee@gmail.com, ³yessayem@yahoo.com

Abstract- Microdischarges are direct current discharges that operate at a relatively high pressure of about 100 Torr and geometric dimensions in the 10-300 micrometer range. Microdischarges sustained at high gas pressure in specific geometries possess several unique properties that can be very stable and useful tools for atomic emission spectrometry, surface treatment, reduction of pollutants, fuel reforming and generation of UV and VUV radiation. Our motivation for the study of microdischarges comes from such potential application of these devices. A particular type of microdischarge, which is the microhollow cathode discharge (MHCD), can be used as an electron source to sustain a larger volume discharge. Here we present results from modelling of 3-electrode microdischarge configuration consisting of a microhollow cathode discharge (MHCD) (used as plasma cathode) and a microcathode sustained discharge (MCSD) (maintained in the volume between the plasma cathode and a third positive electrode). Accurate solutions of the continuity equations, electron energy balance equation and poisson's equation with realistic boundary conditions are obtained using a detailed two-dimensional multi-species continuum (fluid) model. Realistic discharge characteristics are simulated, which are very important to understand the phenomena of microdischarges. The influences of gas pressure on discharge characteristics are also investigated. Most predictions presented in this paper are in qualitative and quantitative agreement with experimental data under similar conditions.

Keywords: DC, Microhollow cathode discharge (MHCD), Microcathode sustained discharge (MCSD), Fluid model, Discharge properties.

1. INTRODUCTION

The microhollow cathode discharge (MHCD) refers to a canonical microdischarge generated in a metal(C)/dielectric/metal (A1) sandwich structure into which a through or blind hole is drilled. The thickness of the sandwich layers and the hole diameter is of order tens to hundreds of micrometers [1]. Microdischarges are being developed to answer the increased interest in generating stable direct-current nonthermal plasmas at high gas pressures. Their operation is stable for gas pressures approaching, or even exceeding, atmospheric pressures, avoiding the glow-to-arc transition. Owing to their advantages of high-pressure operation and high number density, MHCDs have been used in various industrial applications such as etching on flexible structures, [2] oxygen generation, [3] ignition assistance of dielectric-barrier discharge (DBD) [4] or hydrogen generation for a fuel cell [5]. However, due to the small geometric size of MHCDs, practical applications are still limited. Hence, several efforts have been made to increase microdischarge volume. One such microdischarge configuration is the microhollow cathode discharge (MHCD) developed by Stark and Schoenbach

[6]. A 3-electrode configuration consisting of a MHCD and an additional third planar electrode(A2) biased positively, placed some 3 to 10 mm away, can be used to generate a larger plasma volume [6]. A schematic of such a discharge configuration is shown in figure 1.

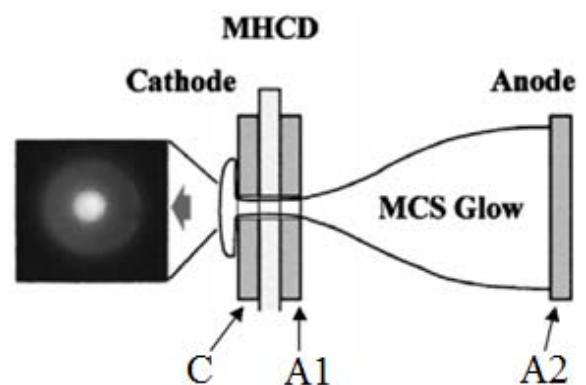


Fig.1: Schematic of microdischarge configuration MCSD with MHCD as electron source [6].

The plasma produced in the volume between MHCD and anode A2 is termed Micro Cathode Sustained Discharge (MCSD). Diagnostics are difficult in these microdischarges because of their small geometric dimension and available experimental data for plasma properties in the volume between the MHCD sandwich and the third electrode are limited [7]. The computer simulation hence becomes an important method to reveal the physics in this microdischarges. A better understanding of the mechanisms that are responsible for the microdischarge stability at high gas pressure requires not only experimental but also extensive theoretical work. In this paper, we describe the general properties of the plasma in the MCS region as deduced from a numerical study. Predicted results are compared to experimental data. The analysis is for the steady state of plasma parameters.

2. GOVERNING EQUATIONS

Governing equations solved in this model are discussed below:

2.1 Species Continuity

The densities of individual species in the discharge are determined by the species continuity equation,

$$\frac{\partial n_k}{\partial t} + \vec{\nabla} \cdot \vec{f}_k = \dot{G}_k + \frac{(n_k^{in} - n_k)}{\tau_{flow}}, \quad k=1 \dots K_g \quad (1)$$

Where n_k is the number density of species of index k (units: #/m³-s), \vec{f}_k is the total species k number flux density, \dot{G}_k is the gas-phase species generation rate through plasma chemical (units: #/m²-s), and K_g is the total number of gas-phase species. The term τ_{flow} is the bulk flow residence time (units: s) and n_k^{in} is the number density of species k in the inlet for the discharge.

2.2 Electron Energy

The electron temperature, T_e , is determined by solution of the electron energy equation which is given as follows.

$$\frac{\partial e_e}{\partial t} + \vec{\nabla} \cdot \{(e_e + p_e)\vec{u}_e + \vec{q}_e\} = S_e \quad (2)$$

Where

$e_e = \left(\frac{3}{2} k_B T_e + \frac{1}{2} m_e u_e^2 \right) n_e \approx \frac{3}{2} k_B T_e n_e$ is the electron volumetric energy (units: J/m³) $p_e = n_e k_B T_e$ is the electron pressure, $\vec{u}_e = \vec{u} + \vec{U}_e$ is the electron total fluid velocity, $\vec{q}_e = -\kappa_e \vec{\nabla} T_e$ is the electron thermal flux (units: J/m²-s) and S_e is the source term on the right hand side of the equation.

2.3 Electrostatic Potential

Poisson's equation given as

$$\nabla \cdot (\epsilon_r \nabla \Phi) = -\frac{\rho_c}{\epsilon_o} \quad (3)$$

Where ϵ_r is the relative dielectric permittivity of the material (here =1 for gas), ρ_c is the space charge density (units: C/m³), and ϵ_o is the dielectric permittivity of vacuum (8.854×10^{-12} F/m).

2.4 Species Momentum

The ion species momentum equation,

$$\frac{\partial n_i \vec{u}_i}{\partial t} + \vec{\nabla} \cdot (n_i \vec{u}_i \vec{u}_i) = -\frac{e Z_i}{m_i} n_i \vec{E} - \frac{1}{m_i} \vec{\nabla} p_i - n_i (\vec{u}_i - \vec{u}) \vec{v}_i \quad (5)$$

Where n_i is the ion number density, m_i is the ion particle mass, \vec{v}_i is the ion species collision frequency, Z_i is the ion charge number, e is unit charge (1.602×10^{-19} C), \vec{E} is the electric field, $p_i = n_i k_B T_i$ is the ion species pressure, and \vec{u}_i is the mean mass fluid flow velocity. The ion temperature is given by T_i .

3. PLASMA CHEMISTRY

A pure argon plasma gas chemistry is used and comprises six species: electrons (e), atomic argon ions (AR⁺), molecular argon ions (AR₂⁺), metastable atoms (AR^m), dimer metastable atoms (AR₂^m), and the background argon atoms (AR). The reactions considered in the study comprises electron impact ionization and excitation reactions, Penning ionization reactions, three-body reactions for dimer excited species and ion formation, quenching and de-excitation reactions. At the surfaces all excited species and charged species are assumed to get quenched with unity sticking coefficient. Upon quenching at surfaces, each dimer ion and excited species is assumed to return to plasma a pair of ground state neutral AR atoms, while the monomer species return as a single AR atom.

4. NUMERICAL DETAILS

The numerical model is based on a cell-centered, finite volume discretization of the discharge governing equations on unstructured meshes. An implicit technique has been implemented for the time differencing of the governing equations. The spatial discretization uses an upwind scheme for the convection-diffusion terms in the species continuity and energy equations. Figure 2 shows the computational mesh and the 2D axisymmetric-Y cylindrical form geometry of the MCSD used in this study. The geometry is consisted of a dielectric/cathode/dielectric/anode/dielectric sandwich through which a cylindrical hole is drilled. A third

positively biased electrode is placed 3 mm away from MHCD. The hole radius is of 300 μm , metal foils (electrodes) of thickness 200 μm , and a dielectric layer thickness of 200 μm . Outer farfield boundaries on the gas subdomain of the discharge are modeled as symmetry. This boundary condition ensures that no secondary discharge is established between the electrodes and the outer boundaries given the finite size of the computational domain. The mesh consists of about 21,329 cells of which about 16,531 are in the plasma (gas subdomain) and about 4,798 are in the dielectric layers (dielectric subdomain). The electrodes are treated as perfect conductors and are therefore not meshed. A combination of triangles and quadrilaterals is used in the plasma region to optimize requirements of solution resolution and cell count. The mesh is refined towards the cathode with quadrilaterals to capture the steep gradients that exist for most solution variables in the cathode sheath. The use of a mixed cell (triangles and quadrilaterals) mesh constitutes a significant advantage compared to a pure triangle or pure quadrilateral mesh [1].

5. RESULT AND DISCUSSION

Electron, monomer ion (AR^+), dimer ion (AR_2^+), and metastable species (AR^m and AR_2^m) number density profiles are shown in Figure 3–4, respectively. The electron density is highest ($n_{e \text{ peak}} = 1 \times 10^{19} \text{ m}^{-3}$ for these conditions) near the exit plane of the MHCD and on-axis due to the expansion of the plasma leaving the MHCD. A plateau region is established on-axis for $(A2-A1) > 1 \text{ mm}$ where densities are approximately constant. These results are consistent with the result estimated by Pitchford et al. [11]. Electron densities in this glow discharge were estimated to be $7 \times 10^{17} \text{ m}^{-3}$ experimentally by Schoenbach et al. [6] in the mid-plane of the main glow discharge, which is in good agreement with our numerical results (10^{18} m^{-3}). The magnitude of the peak electron densities predicted by the model is consistent with the available quantitative experimental data for MHCD in other noble gases [8] and molecular gases [7]. When the gas pressure is

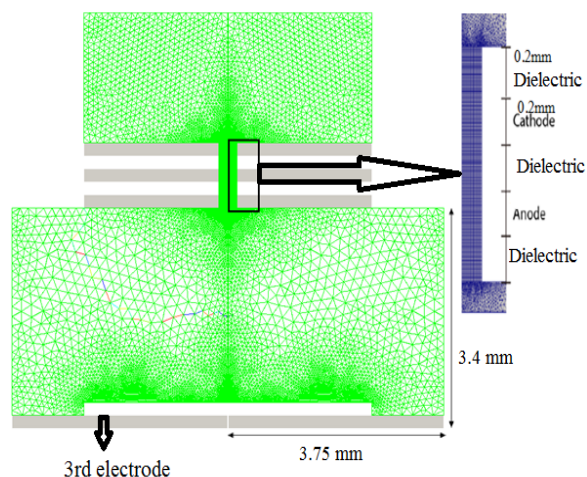


Fig.2: Schematic of the MHCD+MCS device and computational mesh. The geometry is cylindrically symmetric.

increased ($p = 100 \text{ Torr}$), the diffusion of electrons in the radial direction is reduced (Figure 3). The electron density on-axis exceeds $2 \times 10^{19} \text{ m}^{-3}$. The main mechanism of creation of electrons, in the zone of radial expansion of the MCS, is the step-wise ionization, and the losses of electrons are via diffusion in radial direction and dissociative recombination. The peak monomer species density is about $\sim 10^{20} \text{ m}^{-3}$, occurs along the centerline of the hollow and dimer species densities are about $\sim 10^{17} \text{ m}^{-3}$, occurs along the cathode region of the hollow in the MHCD region (Figure 4). Peak value ($1 \times 10^{20} \text{ m}^{-3}$) of metastable atom density in the MCS discharge is one order higher than that of other simulation result [11]. Peak value ($1 \times 10^{19} \text{ m}^{-3}$) of monomer ion (AR^+) density in the MCS zone occurs just in the exit plane of the MHCD which is consistent with other simulation result [7]. Metastable molecules (AR_2^m) are also present in high concentrations which are

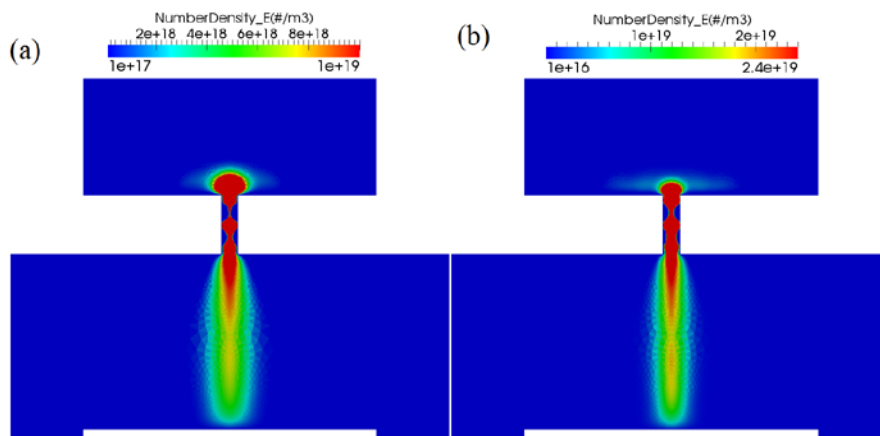


Fig.3: Spatial distributions of the electron density of an MCS. a) At $P=60 \text{ Torr}$. b) At $P=100 \text{ Torr}$.

considered as important constituent for plasma assisted

ignition[9].The gas temperature contours (Figure 5)

indicate non-negligible thermal heating of the gas which is several hundred Kelvin above room temperature. The peak gas temperature occurs along the discharge centerline in the vicinity of the hollow cathode. Recent measurements of the gas temperature in Ar/O₂ mixtures

in the MCS region show that the increase in gas temperature is limited, with a peak temperature at less than 400K over the range of operating conditions of interest [10], which is in again good agreement with our results. Electron temperatures (Figure 6) are highest in

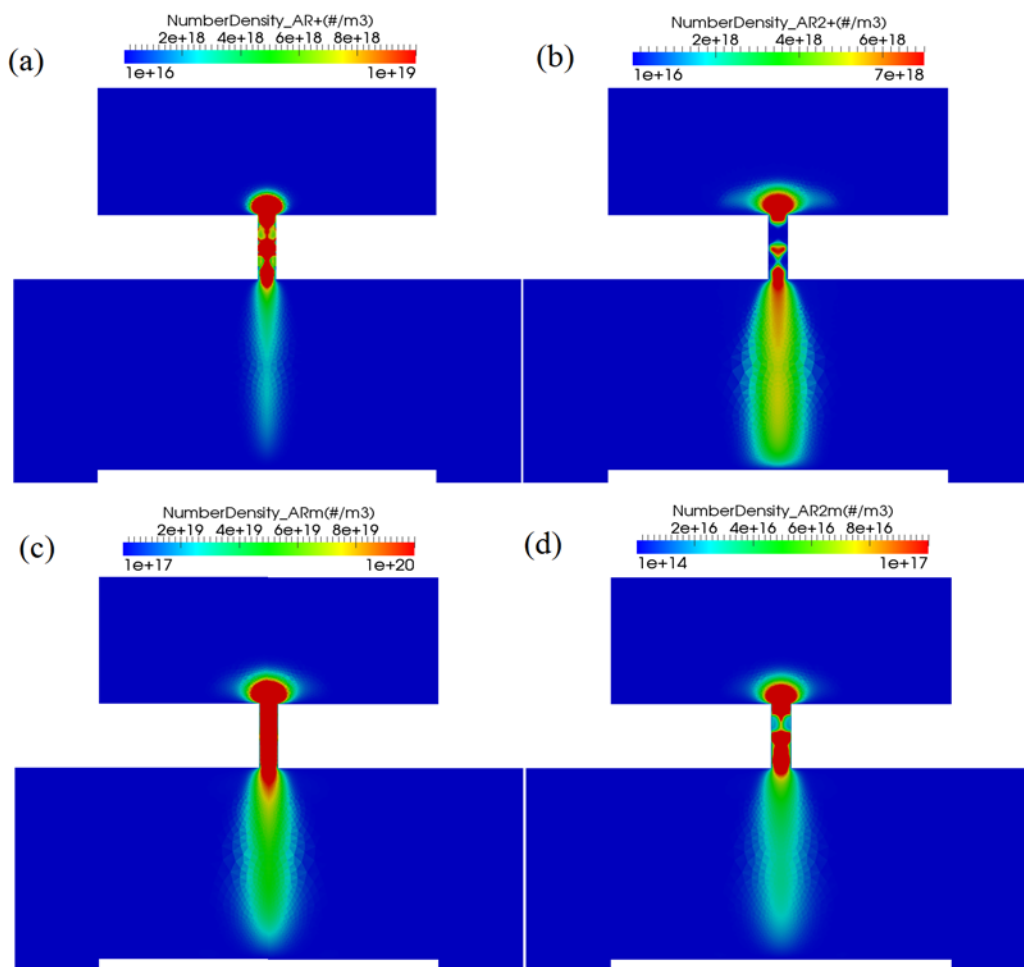


Fig.4: Different species density contours in MCSD. a) Monomer ion (AR⁺). b) Dimer ion (AR₂⁺). c) Metastable atom (AR^m). d) Metastable dimer (AR₂^m).

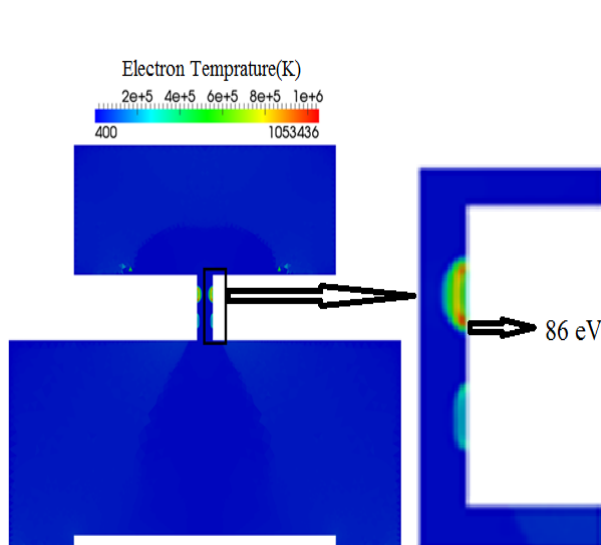


Fig.5: Electron temperature profile

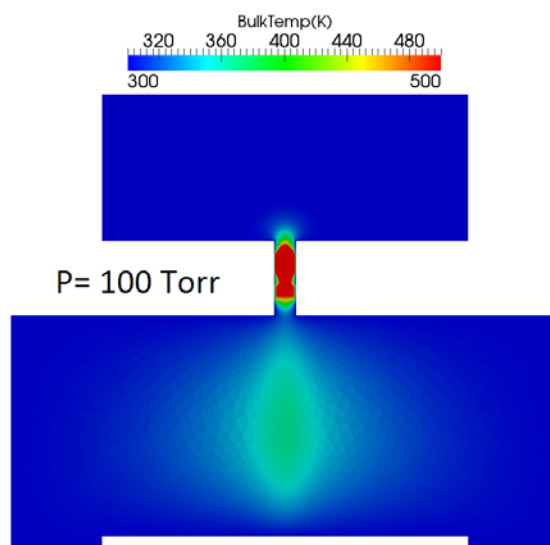


Fig.6: Gas temperature profile

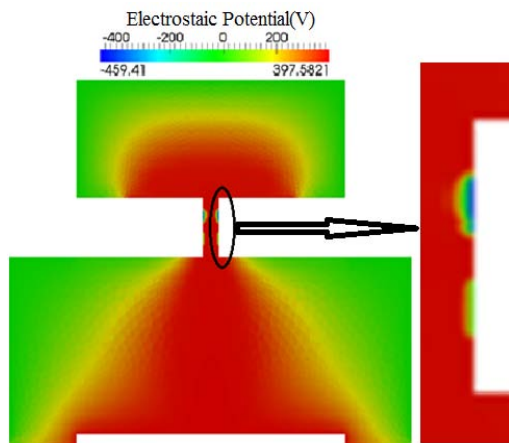


Fig. 7: Electrostatic potential contour

the cathode sheath region within the hollow, with peak electron temperatures on the order of several tens of eV. The electron temperature in the remaining part of the discharge is of order 1 eV. Such high electron temperatures are consistent with what is expected from experimental observations of the emission from high-lying excited states of ionic species in MDs [8]. The characterized regions, i.e., the cathode fall (CF) can be clearly distinguished in the vicinity of cathodes (Figure 7). Most of the potential drops in CF, resulting in a strong electric field. A region of high electric field surrounds the electrode A1, in the proximity of the hole. MHCD acts as a cathode for a larger volume discharge (MCSD).

6. Conclusions

A two-dimensional axis-symmetric, self-consistent multi-species, multi-temperature, continuum (fluid) model is used to estimate different parameters like electrons, ions, metastables and charged particle's number density, and temperature of non-equilibrium high-pressure plasma in this numerical study. The electron temperature reported in this study is as high as expected from experimental observation [8] which is the base of microplasma reactor technology. Charged species densities of order ($e+17 \sim e+19$) m^{-3} and metastable species densities of order ($e+17 \sim e+20$) m^{-3} are predicted for the conditions investigated. In conclusion, simulation results have been presented for a dc microdischarge in a larger volume glow discharges applicable to fuel reforming, gas treatment and surface modification as well. Our model helps one to understand the basic chemical and physical phenomena involved in the MCSD for a particular application.

7. REFERENCES

1. T. Deconinck, S. Mahadevan, L. L. Raja, "Modeling of Mode Transition Behavior in Argon Microhollow Cathode Discharges", *IEEE Trans. Plasma Sci.* 2008, 36, 1200.
2. R. M. Sankaran and K. P. Giapis, "Maskless etching of silicon using patterned microdischarges", *Appl. Phys. Lett.* 79 (2001)

593.

3. G. Bauville, B. Lacour, L. Magne, V. Puech, J. P. Boeuf, E. Munoz-Serrano, and L. C. Pitchford, "Singlet oxygen production in a microcathode sustained discharge", *Appl. Phys. Lett.* 90 (2007) 031501.
4. J. Shin and L. L. Raja, "Microdischarge-assisted ignition of dielectric-barrier high-pressure glow discharges", *Appl. Phys. Lett.* 88 (2006) 021502.
5. H. Qiu, K. Martus, W.Y. Lee, K. Becker, "Hydrogen Generation in a Microhollow Cathode Discharge in High-Pressure Ammonia & #8211; argon Gas Mixtures", *International Journal of Mass Spectrometry*, 233 (2004) 19-24.
6. Stark R H and Schoenbach K H, "1999 Direct current high-pressure glow discharges", *J. Appl. Phys.* 85 2075
7. Leipold F, Stark R H, El-Habachi A and Schoenbach K H 2000, "Electron density measurements in an atmospheric pressure air plasma by means of infrared heterodyne interferometry", *J. Phys. D: Appl. Phys.* 33 2268-73.
8. C. Penache, M. Miclea, A. Brauning-Demian, O. Hohn, S. Schossler, T. Jahnke, K. Niemax, , and H. Schmidt-Bocking, "Characterization of a high-pressure micro discharge using diode laser atomic absorption spectroscopy", *Plasma Sources Sciences and Technology*, 11:476-483, 2002.
9. K. Makasheva, E. Muños Serrano, G. Hagelaar, J.-P. Boeuf, and L. C. Pitchford, "A better understanding of microcathode sustained discharges," *Plasma Phys. Control. Fusion*, vol. 49, no. 12, pp. 233-238, Dec. 2007.
10. J F Lagrange, N Sadeghi, M Touzeau, G Bauville, B Lacour and V Puech, "Gas temperature measurements in a microcathode sustained discharge in oxygen", *Gaseous Electronics Conf (Columbus, Ohio, USA, October 2006)*.
11. K. Makasheva, G. J. M. Hagelaar, J.-P. Boeuf, Th. Callegari, and L. C. Pitchford, "Ignition of Microcathode Sustained Discharge", *IEEE Transactions on Plasma Science*, vol. 36, no. 4, pp.1236-1237, August 2008.

8. NOMENCLATURE

Symbol	Meaning	Unit
n_k	#density of species k	($\#/m^3$ -s)
τ_{flow}	bulk flow residence time	(s)
q_e	electron thermal flux	(J/m^2 -s)
q_c	space charge density	(C/m^3)